

The High Intensity Proton Accelerator Facility

J. Grillenberger¹, C. Baumgarten¹, M. Seidel¹

1 Paul Scherrer Institut, 5232 Villigen PSI, Switzerland

* joachim.grillenberger@psi.ch

July 12, 2021



Review of Particle Physics at PSI
doi:[10.21468/SciPostPhysProc.2](https://doi.org/10.21468/SciPostPhysProc.2)

Abstract

The High Intensity Proton Accelerator Facility at PSI routinely produces a proton beam with up to 1.4 MW power at a kinetic energy of 590 MeV. The beam is used to generate neutrons in a spallation target, and muons, pions and neutrinos in meson production targets. These are used for condensed matter and particle physics research at the intensity frontier. This section presents the main physics and technology concepts utilized in the facility. It includes beam dynamics and the control of beam losses and activation, power conversion, efficiency aspects, and performance figures, including the availability of the facility.

2.1 Introduction

The original proposal for the accelerator facility that is now known as the PSI high intensity proton accelerator (HIPA)¹, was completed 1963 [2]. The objective was to produce a proton beam of several tens of μA with an extraction rate higher than 50% and an energy above 450 MeV, with the main goal to produce π -mesons and muons². The final beam energy was later raised to ≥ 580 MeV and the specified beam current raised to $100 \mu\text{A}$ [3]. The main accelerator is the ring cyclotron, an isochronous proton machine with eight separate magnet sectors and four main accelerating cavities operating at 50.6 MHz. The ring cyclotron is designed to accelerate an injected 72 MeV proton beam to 590 MeV. The first pre-accelerator, called the Injector I cyclotron, was designed and constructed by Philips (Eindhoven). Injector I was a multi-purpose machine, that accelerated protons up to 72 MeV with a maximal extracted current of $I_{max} \leq 100 \mu\text{A}$, and also light ions for nuclear physics research. After one year of operation, in 1975, the highest beam current on target was $25 \mu\text{A}$. The performance of the ring cyclotron was steadily improved, especially the extraction efficiency. In December 1976 an extraction efficiency of 99.9% (Ring) and of 85% (Injector I) was achieved. The peak intensity was raised within two years from $12 \mu\text{A}$ to $112 \mu\text{A}$ [4]. The beam current was limited by the 9% beam losses at the extraction of Injector I and the resulting activation of components. Injector I was also used for low-energy experiments. During these experiments, Injector I was not available as a proton driver for the Ring cyclotron. Injector I was not able to deliver beam currents higher than originally specified, while the performance of the Ring cyclotron indicated the capability for much higher currents with low losses. Therefore, studies for an upgrade of the Ring cyclotron with a flattop cavity and a new injector cyclotron with a Cockcroft-Walton type pre-accelerator for beam currents of up to 1 mA were in progress while

¹Formerly named the *Isochronous Cyclotron Meson Factory of ETH Zurich* [1], then the Schweizerische Institut für Nuklearforschung (S.I.N.) ring Cyclotron.

²The term *meson* production targets was established for historical reasons - even though muons are leptons.

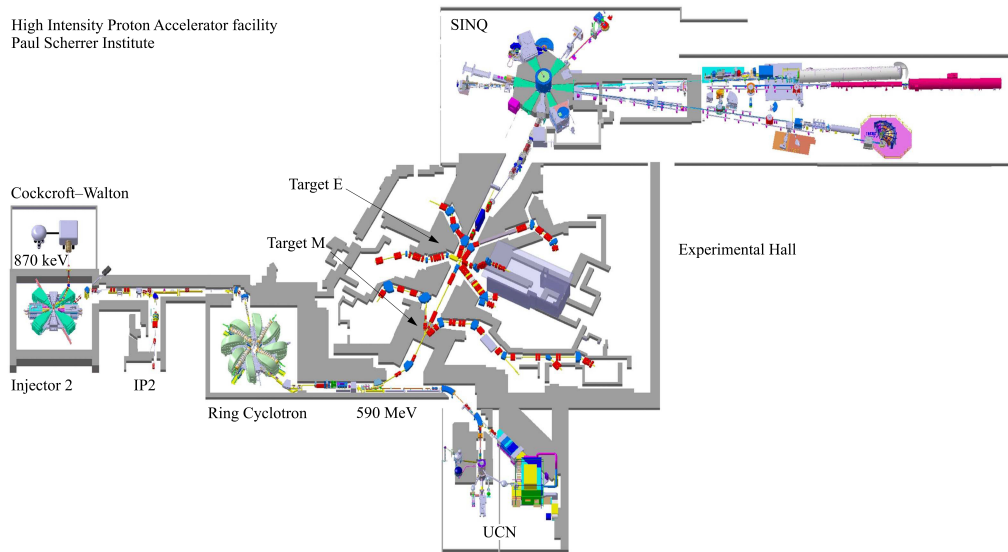


Figure 2.1: Layout of the High Intensity Proton Accelerator facility at the Paul Scherrer Institute.

39 the commissioning was still ongoing [5]. At this stage, it was estimated that the Ring cy-
 40 clotron had the potential to accelerate currents of up to 2–4 mA [6]. The proposal to use two
 41 pre-accelerators, a 860 keV Cockcroft-Walton type accelerator followed by the new Injector II
 42 cyclotron, was approved in 1978.

43 The protons have been produced by a compact small electron cyclotron resonance source
 44 since 2010 with a 60 kV extraction system [7]. Two solenoids are used to focus the extracted
 45 protons onto a collimator. Hydrogen ions (H_2^+ and H_3^+), which are extracted as well, are only
 46 weakly focused due to their lower charge-to-mass ratio, and are stopped. The protons are
 47 accelerated in three stages. A Cockcroft-Walton DC linear accelerator, shown left in Figure 2.1,
 48 is used to pre-accelerate the DC proton beam to 0.87 MeV as required for the injection into the
 49 first turn of the Injector II cyclotron. The beamline is equipped with a bunching system a few
 50 meter upstream of the axial injection line, to match the beam phase space to the acceptance
 51 of Injector II. Injector II accelerates the pre-bunched beam with two high-voltage double-gap
 52 resonators³ ("Dees") to an energy of 72 MeV within 80 turns. The extracted beam is then sent
 53 to an electrostatic beam splitter, where up to 100 μ A can be split off for the production of radio-
 54 isotopes. The main part of the beam is injected into the Ring cyclotron with an electrostatic
 55 inflection channel. Eight normal-conducting magnets keep the particles' almost circular paths
 56 in the cyclotron. Four 50.6 MHz cavities accelerate the beam to its final kinetic energy of
 57 590 MeV. After about 180 turns in the cyclotron, the beam is extracted with an electrostatic
 58 element (see Figure 2.2) and sent to the meson production targets. These production targets
 59 are made of graphite and limited in thickness so that the beam loses only a fraction of its
 60 energy. After passing through a collimation system, needed due to multiple scattering in the
 61 meson production targets, roughly 60 (70) % of the beam current is left for a target thickness
 62 of 60(40) mm, and is then sent to the neutron spallation source SINQ [8–12]. If SINQ is not
 63 ready for beam, the beam is sent to the 590 MeV beam dump. Due to cooling issues, the beam
 64 current is limited to 1.6(2.0) mA on a 40(60) mm thick meson production target. The Ultracold
 65 Neutron Source (UCN) has been in operation since 2011 [13–16]. A fast kicker magnet just
 66 upstream of the meson production targets deflects the beam for a short time between 2 and

³A double-gap resonator is equivalent to a conventional Dee with two accelerating areas (gaps). In contrast the PSI Ring cyclotron uses hollow "single-gap" cavities.

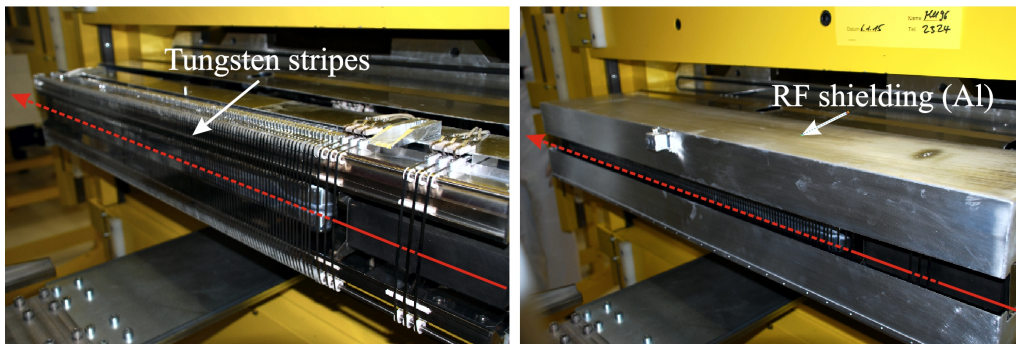


Figure 2.2: Pictures of the electrostatic extraction channel EEC without (left) and with attached aluminum shroud (right). The red arrow denotes the beam passing through the channel. The dashed part of the arrow denotes the parts where the beam passes through in between the grounded tungsten stripes and the aluminum cathode. The electric field of 8 – 10 MV/m deflects the beam by 8 mrad on 920 mm effective length so it can be extracted from the cyclotron by a subsequent septum magnet.

67 8 s to the UCN facility. The duty cycle is restricted to a maximum of 3%.

68 The intention of this article is to present performance figures for the accelerator together
 69 with the main physics and technology concepts utilized in the facility. This includes beam
 70 dynamics and space charge effects in the cyclotrons, the control of beam losses and activation,
 71 power conversion, and efficiencies. While some of these topics are relevant only for cyclotrons,
 72 many themes are discussed that are important for any type of high intensity proton accelerator.
 73 In the following sections, the basic physics and main parameters of the three accelerators are
 74 described.

75 2.2 Injector II

76 The Injector II cyclotron was designed for high current operation, 1 mA and above, with min-
 77 imal extraction losses. High extraction efficiency in a cyclotron demands a large turn separa-
 78 tion. This can be achieved by the combination of high accelerating voltage, large radius, large
 79 gap magnets and low energy spread. To counter the strong defocusing space charge forces, a
 80 high vertical ("axial") betatron-tune⁴ is required. Hence Injector II was designed as a low-field
 81 separate sector machine using four wedge sectors. The sector magnets leave space for two
 82 high-voltage double-gap resonators operating at the 10th harmonic of the orbital frequency
 83 and two single-gap flat-top resonators to minimize the energy spread. Since the injection
 84 energy of 870 keV is well below the Coulomb threshold, the first few turns can be used to
 85 collimate the beam and clean up halo [17].

86 M.M. Gordon was the first to recognize that space charge in isochronous cyclotrons can lead
 87 to (as he called it) "vortex motion" [18]. Later Chabert, Luong and Promé as well as Chasman
 88 and Baltz backed this up theoretically [19, 20]. Numerical simulations, performed by Adam,
 89 Koscielniak, Adelmann and others, confirmed this effect [21–24]. The vortex effect can lead
 90 to increased halo formation and bunch "breakup". This has been experimentally investigated
 91 by Pozdeyev *et al* in the *small isochronous ring* (SIR) experiment [25]. The beam breaks up
 92 only if it is long initially and the breakup typically generates a number of self-sustaining round
 93 sub-bunches [25]. In case of a single initially short and compact bunch, the vortex effect stabi-
 94 lizes the bunch: the space charge induces a coupling between the longitudinal and horizontal

⁴The "tune" is the number of vertical or horizontal oscillations of a particle per turn and characterizes the strength of vertical/horizontal focusing. Isochronous cyclotrons have, in contrast to synchrotrons, no intrinsic longitudinal focusing.

95 motion that generates a weak (but non-zero) longitudinal focusing, an effect that can be under-
96 stood with an analysis of the linear coupling terms of an isochronous cyclotron [26], although
97 this is somewhat counter-intuitive. The usefulness of the self-focusing was discovered by the
98 PSI operation crew, who achieved a high extracted current with low losses while the flat-tops
99 were switched off by accident. Since the flat-top system was –with an appropriate setup– no
100 longer required to achieve a low energy spread, the phase was reversed so as to operate in
101 an accelerating mode. This enabled a further increase in the energy gain per turn and hence
102 to reduce the turn number N . A maximum beam current of 2.7 mA has been extracted from
103 Injector II on beam dump and 2.4 mA in combination with the Ring cyclotron.

104 The flat-top resonators will be replaced, in an ongoing upgrade program, by two 50 MHz
105 high-voltage resonators. This should further reduce extraction losses and allow for even higher
106 beam currents. However, the vortex effect generates bunches in a meta-stable state and is sen-
107 sitive to various possible distortions [27, 28]. Making use of the vortex effect in Injector II
108 may be possible due to the very conservative layout of the cyclotron, including a strict isochro-
109 nism, [26] with a central region equipped with various movable collimators to optimize the
110 bunch formation and to eliminate the halo [17]. Injector II is the only production cyclotron
111 world-wide that is known to take advantage of the vortex effect.

112 2.3 The Ring Cyclotron

113 In 1975, after one year of operation, the highest beam current on target was $25 \mu\text{A}$. The perfor-
114 mance of the Ring cyclotron was steadily improved, especially the extraction efficiency. In the
115 beginning, only a well-centered beam was able to pass the Walkinshaw-resonance without sub-
116 stantial beam loss, as the beam had to pass the resonance four times before extraction [5, 29].
117 A modification of the tune diagram by an improved setting of trim coils reduced this to two
118 fast passages through the resonance and allowed relaxation of the requirement of beam cen-
119 tering [30, 31]. This enabled a considerable increase in the turn separation at extraction by
120 means of precessionally-enhanced turn separation. In December 1976 an extraction efficiency
121 of 99.9% was achieved with a peak intensity of $112 \mu\text{A}$ [4]. Ten years later, after the first com-
122 missioning of the new pre-accelerators, a beam current of 1 mA was extracted from Injector II
123 and $310 \mu\text{A}$ from the Ring cyclotron.

124 In 1981, Werner Joho presented an analysis of high intensity problems in cyclotrons [32],
125 known as Joho’s N^3 -Law, which states that the loss dominated current limit I_{max} scales with
126 the inverse third power of the number of turns N , $I_{max} \propto N^{-3}$. This formula predicted the
127 performance of the PSI Ring cyclotron of the following two decades with high accuracy [33,
128 34].

129 An upgrade of the RF system of the Ring was required and initiated for another substantial
130 intensity increase [35]. In parallel, a bunching system was built and commissioned in the
131 870 keV injection line to better match the DC beam to the phase acceptance of Injector II [36,
132 37]. The upgrade of the RF system allowed a significant reduction of the number of turns in
133 the Ring cyclotron and an increase of the production current to 2.2 mA (test-wise in dedicated
134 shifts up to 2.4 mA) and the beam power to 1.3 MW (1.4 MW), in good agreement with Joho’s
135 N^3 -Law (see Figure 2.3). On full completion of the upgrade programs, which includes the
136 replacement of the old 150 MHz flattop cavity, a beam current of 3 mA with a power of 1.8 MW
137 should be within reach of both, Injector II [17] and the Ring cyclotron [38, 39].

138 2.4 Facility Performance

139 Every year, PSI has 1500-2000 user visits at the neutron source (SINQ), the muon source ($S\mu S$),
140 and the facilities for particle physics (CHRISP) including the UCN Source. During more than
141 3000 instrument-days, over 800 experiments are performed each year. These user facilities

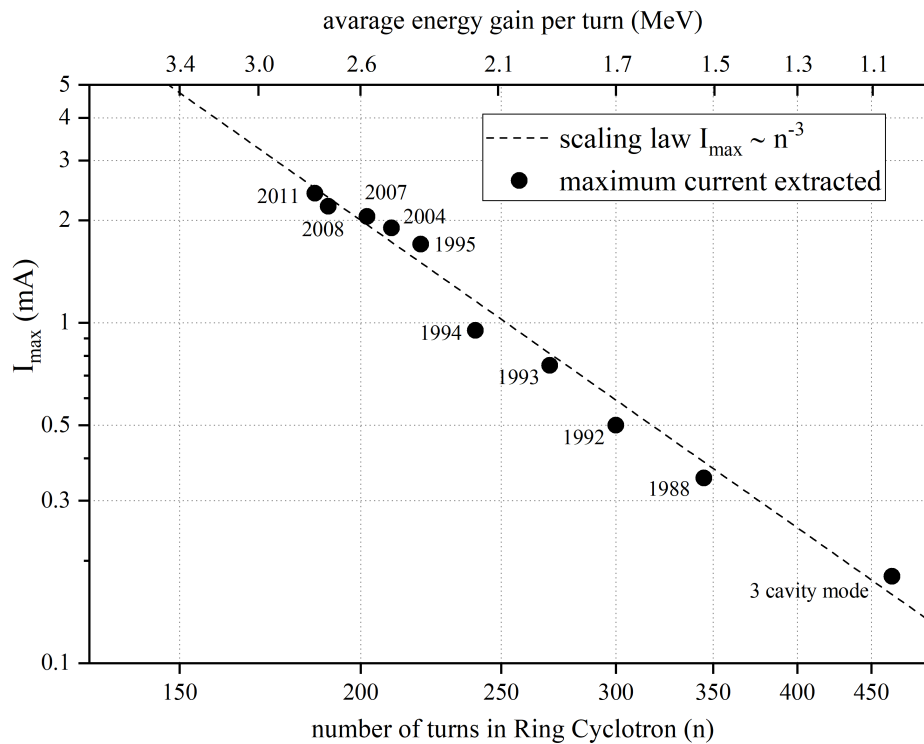


Figure 2.3: Joho's empirical law.

142 are all part of the HIPA facility which operates at a beam power of up to 1.42 MW. In the
 143 following sections we describe the basic operation scheme of the facility and present the main
 144 details of the experimental stations. The performance of the accelerator, i.e., the achievable
 145 beam power, the availability, and its energy efficiency are also addressed.

146 2.4.1 Operation Scheme

147 A typical year of operation starts in the beginning of May after a shutdown starting in January.
 148 The start of user operation may vary depending on the duration of the necessary maintenance
 149 and planned upgrade. The beam time schedule is compiled by the facility management in
 150 close collaboration with the user office of PSI. During regular user operation, the accelerators
 151 are operated nonstop for 24 hours the day. With the user operation starting in the beginning
 152 of May and ending at Christmas, the accelerator facility typically provides 200 days of primary
 153 beam for experiments. After three weeks of user operation, a maintenance period of two days
 154 is scheduled. In addition, two shifts of beam development before and after each maintenance
 155 are carried out to reduce beam losses and to improve the performance of the facility.

156 2.4.2 Pion and Muon Production

157 The production of pions and muons is possible with beam sent either to the spallation neu-
 158 tron target or to the beam dump. In the latter case, the maximum beam current extracted
 159 from the Ring cyclotron is limited to 1.7 mA due to the cooling limitations of the beam dump.
 160 Nevertheless, meson production is possible even though the spallation source may not be op-
 161 erational. The meson targets provide secondary particles for the experimental facilities. The
 162 performance of the meson facilities, i.e., the particle fluxes are given in Table 2.1.

Table 2.1: Particle types available at the meson experimental facilities. The rate is given in particles per second and per mA beam current and may vary with the selected momentum.

Target (thickness)	User facility	Particle type	Momentum range (MeV/c)	max. rate ($s^{-1}mA^{-1}$)
M (5mm)	$\pi M1$	$e/\pi/\mu/p$	10 – 500	$2 \cdot 10^8$
	$\pi M3.1-3$	μ	10 – 40	$3 \cdot 10^6$
E (4 or 6cm)	$\pi E1$	$\pi/\mu/p$	10 – 500	$1 \cdot 10^9$
	$\pi E3$	μ	10 – 40	$3 \cdot 10^7$
	$\pi E5$	π/μ	10 – 120	$5 \cdot 10^8$
	$\mu E1$	μ	60 – 120	$6 \cdot 10^7$
	$\mu E4$	μ	10 – 40	$4 \cdot 10^8$

163 2.4.3 Neutron production

164 The main beam passes through the two graphite targets before striking the spallation neutron
 165 target of SINQ so it has to be collimated due to a five-fold increase in beam emittance. For an E-
 166 target thickness of 4(6) cm, about 70%(60%) of the beam current remains. The proton kinetic
 167 energy is degraded to 570 MeV (565 MeV). The remaining beam is first bent downwards and
 168 then sent back up vertically onto the spallation target. The thermal neutron flux scales with
 169 the beam current and is approximately $1.5 \cdot 10^{14} \text{ cm}^{-2}\text{s}^{-1}$ near the target.

170 The UCN facility was commissioned in 2010 and a measurement of the neutron electric
 171 dipole moment, nEDM, began in 2011. For this experiment, the full 590 MeV beam is switched
 172 periodically from the meson production targets to the UCN target with a fast-switching magnet.
 173 Typically, the beam is switched every 12 minutes for 8 seconds. Both the pulse duration and
 174 frequency can vary depending on the requirements of the experiments. This corresponds to a
 175 duty cycle of approximately 1%. The pulse sequence is controlled by a software routine that
 176 decreases the beam intensity by 20% roughly 2s before the kick. After switching on the kicker
 177 magnet, the maximum intensity is then re-set to the nominal value during another 2s. The
 178 reverse routine applies after the kick.

179 When the beam is switched back to the meson production and SINQ targets, the beam
 180 current is lowered below 1 mA and then raised back to the maximum within 20s. This is done
 181 to avoid high thermal stress to the targets, particularly the SINQ-target.

182 2.4.4 Isotope Production

183 The Injector II Cyclotron can produce 72 MeV protons for the production of radioactive iso-
 184 topes. Two operating modes are possible: An electrostatic beam splitter can split up to $100 \mu A$
 185 of the main beam, which is directed to the isotope production target along a dedicated beam-
 186 line. In this case, both the isotope production beam and main beam onto meson and neutron
 187 production targets can operate simultaneously. Alternatively, the full beam, limited to $100 \mu A$,
 188 can be sent to the isotope production target.

189 2.4.5 Accelerator Performance and Beam Intensity

190 The facility, designed for a maximum beam current of $100 \mu A$, has continuously been improved
 191 to reach a maximum beam power of 1.42 MV, at present. The following section describes
 192 the performance characteristics of the accelerator facility, in particular the beam power and
 193 availability.

194 The maximum beam power is limited by the tolerable amount of proton losses during
 195 acceleration to meet legal obligations and to avoid activation and damaging of accelerator

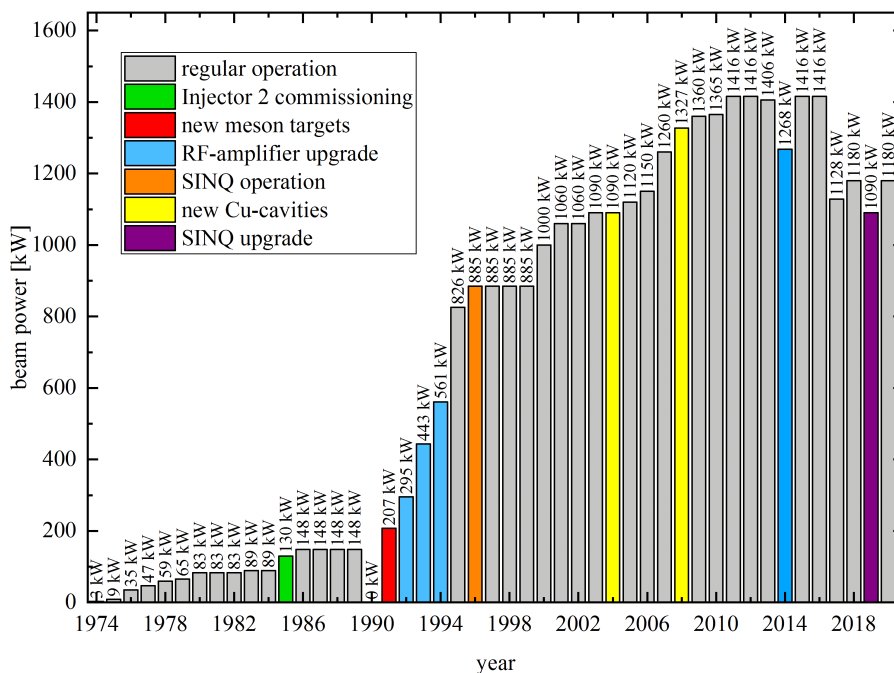


Figure 2.4: The maximum beam power achieved in the accelerator facility. In 1990 the facility was off line for the installation of new RF-amplifiers for the Ring cyclotron and the new meson production target station E including the beamline up to the beamdump.

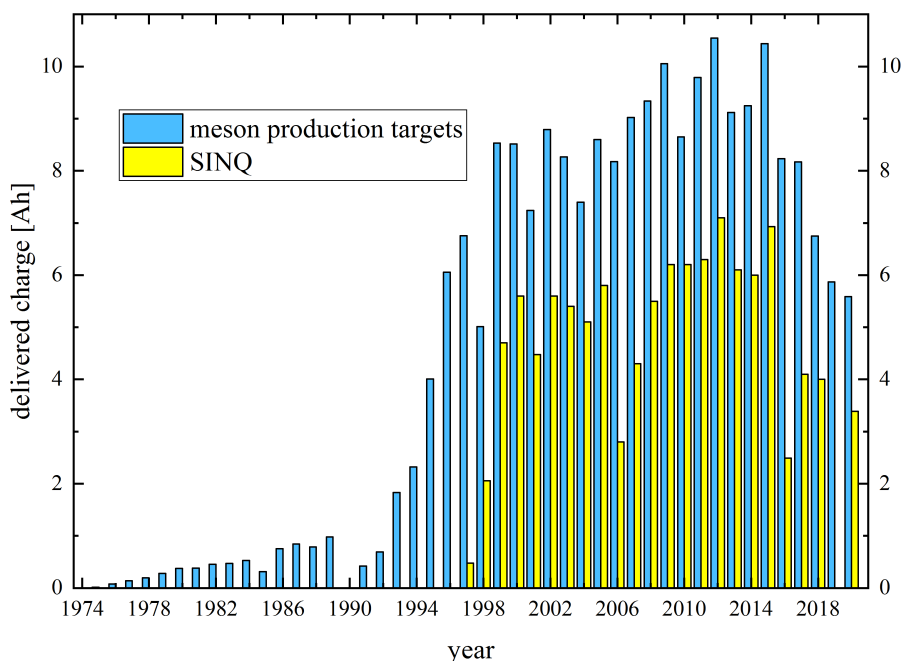


Figure 2.5: History of the charge delivered per year to the meson production targets and the neutron spallation target SINC.

196 components. Currently, PSI is authorized to extract a maximum beam current of 2.4 mA from
 197 the Ring cyclotron, which has been achieved in the years 2011, 2012, 2015, and 2016. Fur-
 198 thermore, PSI may increase the beam current to a maximum of 2.6 mA during dedicated beam
 199 development shifts for eight hours every four weeks. Major steps in the increase of the beam
 200 power were achieved by replacing the Injector I Cyclotron with the Cockcroft-Walton and In-
 201 jector II pre-accelerators in 1985, and by continuous upgrades of the RF systems starting in
 202 1990. Newly designed meson production targets have been used since 1991 to tolerate the
 203 thermal stress imposed by the higher beam power. After the commissioning of the spallation
 204 neutron target SINQ in 1996, the beam power was increased from 826 to 885 kW.

205 Following the installation of last new copper cavity in the Ring cyclotron, the beam losses
 206 in the cyclotron were further reduced by increasing the peak voltage of each accelerating cavity
 207 from 790 MV to 850 MV. A maximum beam current of 2.4 mA was extracted on 20 June 2011
 208 for the first time. The corresponding beam power of 1.42 MW was the highest ever achieved
 209 with any accelerator at that time. In Figure 2.4, the increase of the beam power for the years
 210 from 1974 to 2020 is shown.

211 The charge delivered on the meson and the neutron production targets scales with the
 212 average beam current extracted from the Ring cyclotron and is shown in Figure 2.5.

213 The beam intensity in HIPA is limited by beam losses. As practical experience has shown,
 214 the highest acceptable losses for hands-on maintenance are of the order of 100 W (10^{-4} for
 215 1 MW of beam power) per location. A major contribution is scattering of halo particles in the
 216 high voltage electrode of the extraction septum. Such losses are then distributed over several
 217 meters of beamline elements and lead to activation with maximum dose rates of the order
 218 of 10 mSv/h. Such dose rates of a few mSv/h are acceptable for service work and handling
 219 components. To further increase the beam current, the relative losses in the cyclotron and the
 220 beam line would have to be reduced inversely proportional to the intensity to keep the activa-
 221 tion at an acceptable level. The extremely high extraction efficiency of the PSI Ring cyclotron
 222 is a property that was optimized to allow the operation with high intensities. There are two
 223 key elements for low loss beam extraction: The generation of beam tails must be suppressed
 224 as best as possible, and the turn separation at the extraction septum must be maximized. In
 225 this way the density of halo particles at the position of the extraction septum is minimized. For
 226 an isochronous cyclotron the radial increment of the orbit radius per turn can be computed as

$$\frac{dR}{dn_t} = \frac{U_t}{m_0 c^2} \frac{\gamma R}{(\gamma^2 - 1) \nu_r^2}. \quad (2.1)$$

$$= \frac{U_t}{m_0 c^2} \frac{R}{(\gamma^2 - 1) \gamma}. \quad (2.2)$$

227 Here γ is the relativistic energy factor, ν_r the radial tune and U_t the energy gain per turn
 228 and m_0 the rest mass of the proton. Clearly a high acceleration voltage helps, but one finds
 229 a very strong reduction with γ for higher energies. Equation (2.1) illustrates the possibility
 230 to influence the turn separation by weaker focusing over the outer turns of the cyclotron.
 231 This violates the isochronous condition and is therefore only possible over a small number of
 232 turns. The second line (2.2) is the more general relation, for which $\nu_r \approx \gamma$. We also note the
 233 scaling with the extraction radius R , i.e. the size of the cyclotron. With an extraction radius of
 234 4.5 m, the PSI Ring cyclotron is one of the largest cyclotrons in the world. An effective way to
 235 increase the turn separation at the extraction element is the introduction of orbit oscillations
 236 by deliberately injecting the beam slightly off centre. When the phase and amplitude of the
 237 orbit oscillation are chosen appropriately, and the behaviour of the radial tune is controlled
 238 in a suitable way, the beam separation can be increased by a factor of three. This gain is
 239 equivalent to a cyclotron three times larger and is thus significant. Figure 2.6 illustrates how
 240 this scheme is used in the PSI Ring cyclotron. In [40], the beam profile in the outer turns

241 was computed numerically for realistic conditions, and the results are in good agreement with
242 measurements.

243 In Figure 2.7 the frequency of beam losses at a certain current is depicted for the user
244 operation at 2 mA in 2010 and at 2.2 mA in 2015.

245 2.5 Operating Statistics

246 High beam power is important for precise measurements of short duration. However, the
247 availability of a large research facility is often of even greater importance to users. In this
248 section, we describe beam time statistics and outage characteristics.

249 The availability of the HIPA facility requires a beam current of at least 1 mA extracted
250 from the Ring cyclotron during scheduled user operation. According to this definition, the
251 accelerator availability is 100 % if the beam current measured at the meson production target
252 is equal or greater 1 mA. The lower limit of 1 mA is used to meet the needs of the experimental
253 facilities, which require at least this current for performing meaningful measurements. A beam
254 current of least 700 μA onto the spallation target is required for neutron experiments. This
255 corresponds to 1 mA of beam current extracted from the Ring cyclotron. The lowest beam
256 current considered as useful for the user community has been raised from 150 μA to 1000 μA
257 in 2001. An outage of the spallation neutron target SINQ does not affect the availability of
258 the accelerator since the collimated beam after the graphite targets can be sent onto the beam
259 dump. Figure 2.8 shows the availability from 1974 and 2020.

260 A short interruption refers to outages lasting less than five minutes. The average number
261 of short interruptions per year is roughly 15000, but it varies by more than a factor of seven
262 as shown in Figure 2.9.

263 After the replacement of the first aluminum cavity with a copper cavity in the Ring cy-
264 clotron in 2005, major problems were experienced with the electrostatic elements in the cy-
265 clotron. Stable operation was not possible during the first month after the yearly shutdown.
266 Frequent discharges, especially of the electrostatic injection device, made it impossible to tune
267 the accelerator to sufficiently high beam currents. The injection device had to be replaced
268 several times due to damage to the insulators supporting the cathode, caused the discharges.
269 RF-power decoupled from the new copper cavity was causing the problems. Two different ef-
270 fects were determined to induce the discharges. On the one hand, RF-power decoupled from
271 the cavity is absorbed by the electrodes of the electrostatic element which leads to the accu-
272 mulation of charge on the electrodes, creation of halos, and secondary electron emission. In
273 2014 on the other hand, the high amount of short interruptions was mainly caused by plasma
274 phenomena in the Ring cyclotron. The decoupled RF-power from the flattop cavity resonantly
275 excites secondary electron emission in between the magnet poles of the neighbouring sector
276 magnet. These electrons in turn hit the surface of the trim coils of the magnet and produce
277 ions that stray in the vacuum chamber and are attracted by the electric field of the electrostatic
278 elements. This leads to vapor deposition of conductive material on the insulators that support
279 the cathode and thus discharges of the electrostatic elements. To mitigate this effect, an alu-
280 minium shroud was attached to the electrostatic devices to shield the RF-power and screen it
281 from straying ions.

282 Though recovery from a discharge of the electrostatic elements may occur within several
283 milliseconds, the automatic ramping up of the accelerators lasts between 20 to 30 seconds.
284 Therefore, short interruptions may have a non-negligible impact on the yearly availability.
285 Assuming an average of 15000 short interruptions per year the aggregate downtime constitutes
286 approximately 80 hours. Given 5000 hours of user operation, this results in a loss of availability
287 of 1.6 %

288 In Figure 2.10, the accumulated outage characteristics for 2004 through 2020 are shown.
289 The most prominent events causing outages are site cooling (15 %), radio frequency systems

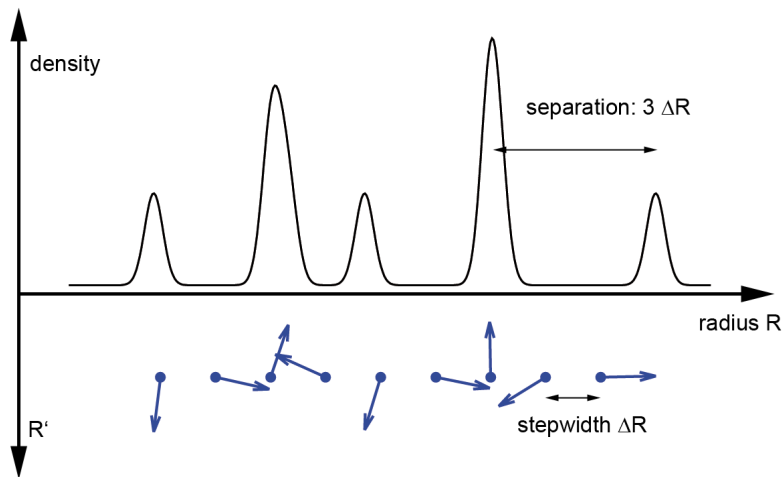


Figure 2.6: Principle scheme of betatron oscillations of the center of the beam around a closed orbit can be utilized to maximize the beam separation at extraction. Important is only the relation between turn-separation and beam width. The 'stepwidth' ΔR is the distance between turns for betatron amplitude zero. The upper plot shows the beam density along the radius, which is a superposition of Gaussian profiles. In the lower half, the clockwise-rotating phase space vector of the centroid of the beam is shown for each turn. The reduction of the radial tune to ≈ 1.5 on the last turns is essential for the intended operation of this scheme.

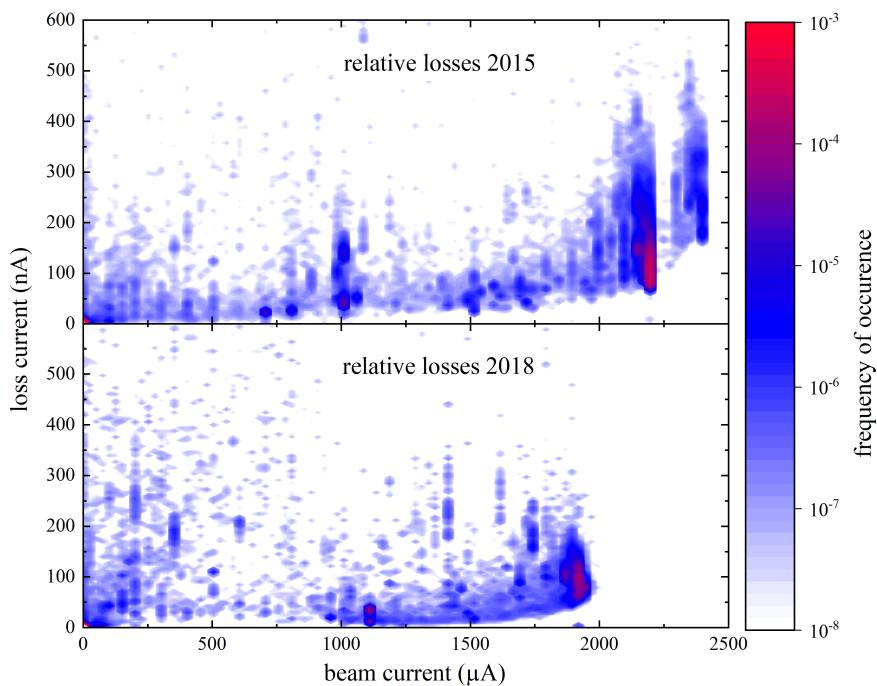


Figure 2.7: Relative losses in the Ring cyclotron during two different operation scenarios. The upper graph depicts the relative losses during the operation in 2015 with a beam current of 2.2 mA for standard operation and 2.4 mA for beam development shifts, respectively. The average loss current at 2.4 mA is approx. 230(44) nA and thus two times higher than at 2.2 mA. Due to the Injector II upgrade, the beam current was limited to 2.0 mA in 2018. The average losses at this current are approx. 82(25) nA

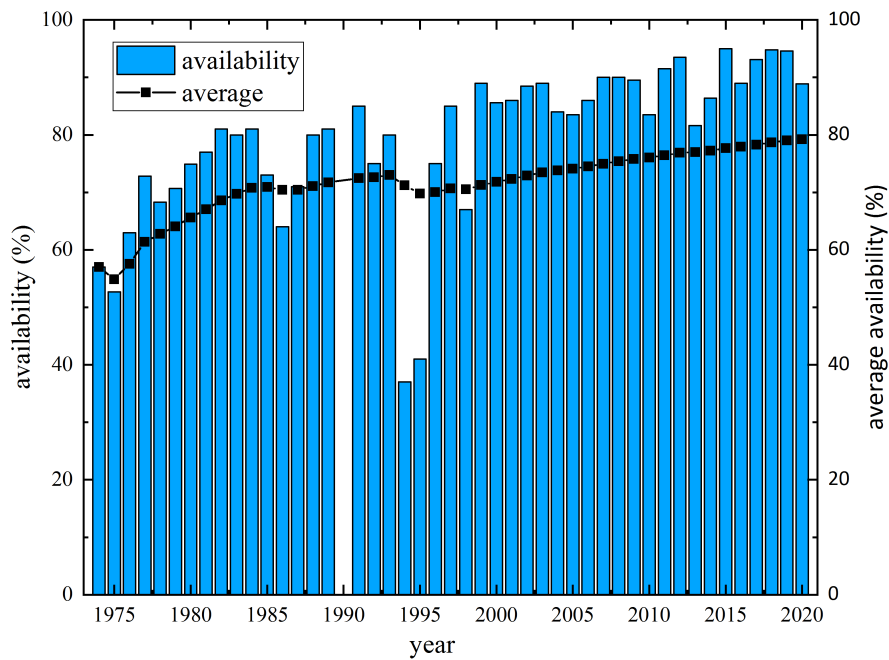


Figure 2.8: Availability of the high intensity proton accelerator facility for the years from 1974 and 2020. The black curve represents the average availability.

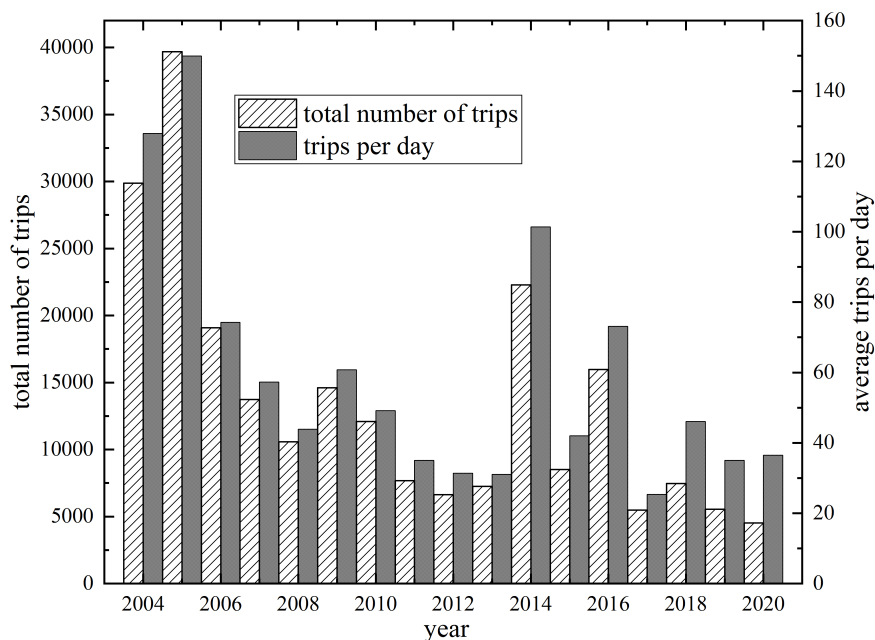


Figure 2.9: Total number of short interruptions for the years 2004 to 2020 (hatched). The solid bars denote the relative number of short interruptions normalized to the number of scheduled days of user operation, i.e., average number of short interruptions (< 5 min.) per day.

290 (13%), and targets (12%). Although this does not reflect the characteristics related to each year of operation, it is a guideline for risk management and stock-keeping of spares.

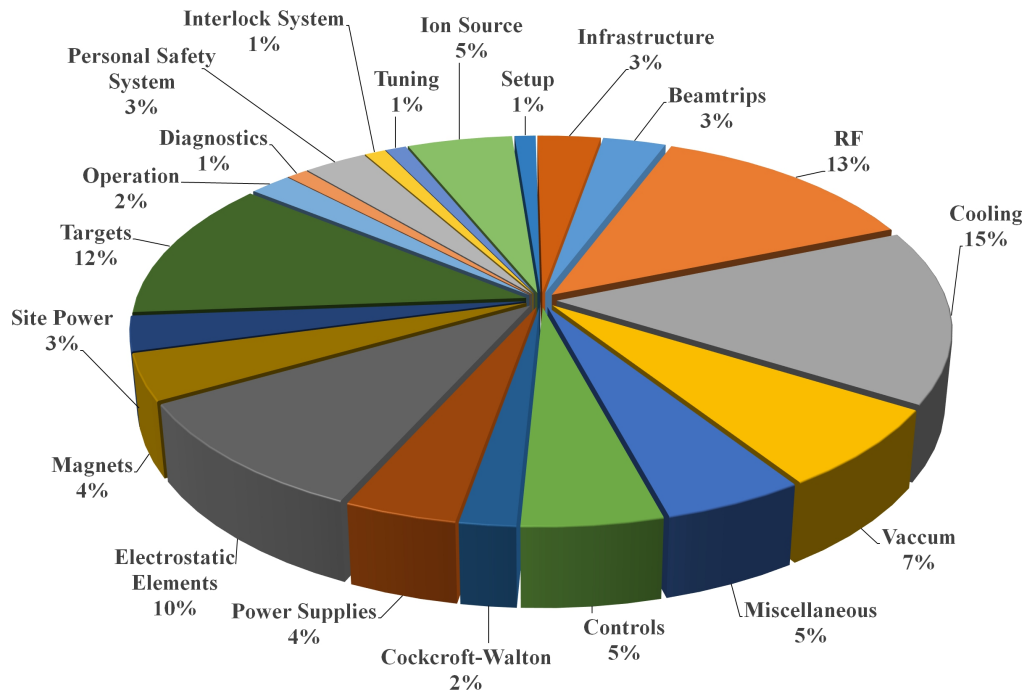


Figure 2.10: Accumulated outage characteristics for the High Intensity Proton Accelerator facility for the years 2004 to 2020.

291

292 2.6 Grid Power Consumption and Energy Efficiency

293 The experiments at HIPA require highest intensity particle beams for precise measurements.
 294 Producing a megawatt proton beam requires the consumption of several megawatts of electrical
 295 power. The goal of further upgrades will be to achieve higher particle flux, rates, bright-
 296 ness, and luminosity, which will require even greater power. Concurrently, the growing global
 297 energy consumption challenges the energy efficiency of any technology including accelerator-
 298 driven research facilities. Inevitably, a discussion on improving the energy efficiency of the
 299 existing facility presents itself. In this section, the energy efficiency of HIPA will be discussed
 300 in detail. Furthermore, it will be shown that by increasing the beam power an even higher
 301 energy efficiency may be achieved.

302 Figure 2.11 shows the power consumption break down of the proton facility. The overall
 303 power consumption of the facility in routine operation at 2.2 mA beam current is approximately
 304 12.5 MW. The 5.4 MW the RF-to-beam power conversion dominates the power consumption.
 305 This value scales roughly linear with beam power (see Figure 2.12): the power consumption
 306 of the magnets and auxiliary systems, e.g., cooling, conventional systems, and instruments is
 307 virtually independent of the beam power.

308 With a beam power of up to 1.3 MW and a total power consumption of 12.5 MW, the en-
 309 ergy efficiency of the facility is 11%. This does not reflect the energy efficiency of the bare
 310 accelerator, as all experimental facilities (IP2, UCN, SINQ, and all secondary beamline experi-
 311 ments) that require electrical power contribute to the total power consumption. In a detailed
 312 study [41], the power consumption of each subsystem (RF-System, magnets, and infrastruc-
 313 ture) required only for beam production, was analyzed. According to this study, a minimum
 314 of 7.12 MW of power from the power grid is required for a beam current of 2.2 mA. Thus, the

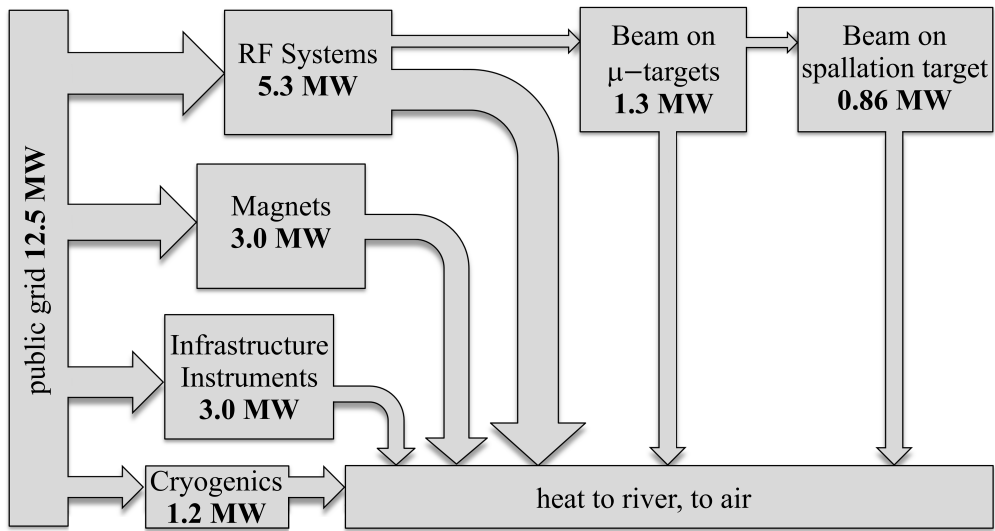


Figure 2.11: Breakdown of the power flow in the Proton Accelerator facility for a beam current of 2.2 mA.

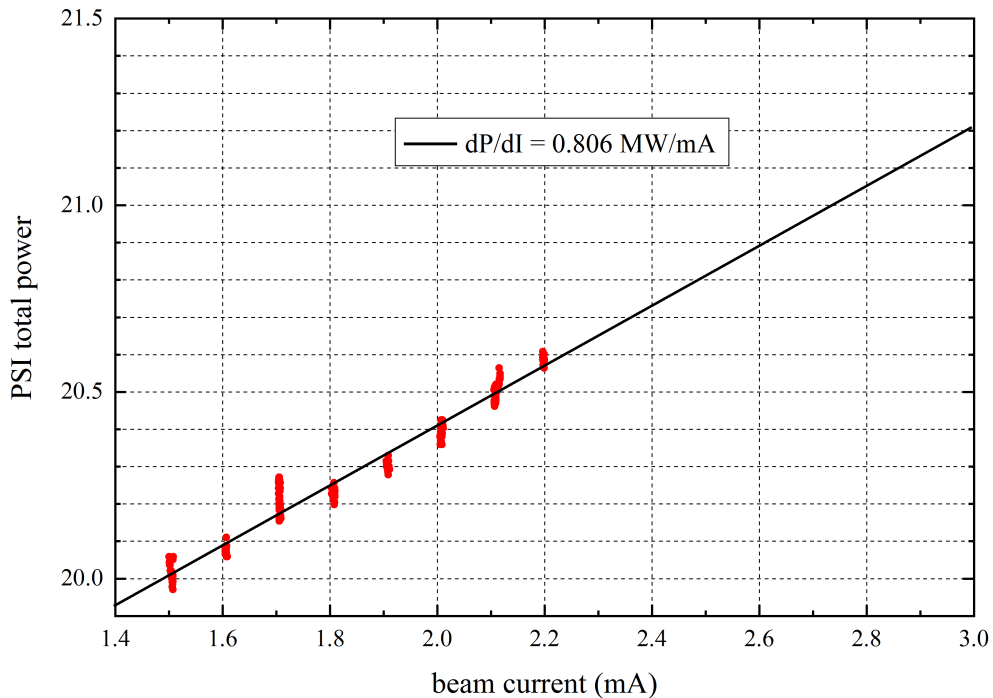


Figure 2.12: Grid to beam power conversion as a function of the beam current. The measurements (red) were recorded with a fixed cavity voltage of each 850 kV. The black line denotes a linear regression of the data. Extrapolated to 3 mA of beam current, a power of 21.2 MW from the grid would be needed.

315 energy efficiency of the bare accelerator is 18%. One might expect the energy efficiency of
 316 the facility to increase linearly with beam power, corresponding to the linear behavior of the
 317 RF- to beam power conversion denoted in Figure 2.12. However, the power consumption P_{RF}
 318 of the RF-System was measured as a function of the beam current keeping the voltage of the
 319 accelerating cavities constant (850 kV per cavity). According to the empirical law of Joho [32]
 320 the number of turns in a cyclotron has to be reduced to achieve higher beam currents. This,
 321 in turn, is only possible by increasing the peak voltage V_{acc} of the accelerating cavities. Since
 322 the wall losses P_{loss} in a cavity scale with $V_{acc}^2/2R$ (where R is the shunt impedance of the cav-
 323 ities), correspondingly more electrical power is needed to increase the beam current. Since
 324 $P_{RF} = P_{loss} + k \cdot P_{beam}$ where k is the efficiency of the RF-amplifier chain, this results in a
 325 non-linear behavior of the RF- to beam power conversion. The considerations in the following
 326 section will proof that increasing the beam current by reducing the number of turns in the
 327 cyclotron will nevertheless increase the energy efficiency of the accelerator facility.

328 The efficiency η_{acc} of the bare accelerator is defined as the ratio of the beam power P_{beam}
 329 and the total power P_{tot} needed to operate the accelerator. In a simplified model, P_{tot} is
 330 $P_{loss} + k \cdot P_{beam} + P_{aux}$. The power consumption P_{aux} of the magnets and auxiliary system, e.g.,
 331 cooling, conventional systems, and instruments is virtually independent of the beam power.
 332 Therefore, the efficiency of the accelerator is

$$\eta_{acc} = \frac{P_{beam}}{P_{loss} + P_{aux} + k \cdot P_{beam}}. \quad (2.3)$$

333 As the maximum current I_{max} extracted from a cyclotron is proportional to $1/N^3$ [32], the
 334 number of turns N is

$$N = \frac{E_{kin}}{q \cdot V_{acc} + P_{aux} + k \cdot P_{beam}}, \quad (2.4)$$

335 where E_{kin} is the kinetic energy of the particles and q their charge. Thus

$$I_{max} \approx \frac{q^3 \cdot V_{acc}^3}{E_{kin}^3} \text{ and } V_{acc} \approx \frac{E_{kin}}{q} \cdot \sqrt[3]{I_{max}}. \quad (2.5)$$

336 The efficiency of the accelerator as a function of the beam current can then be deduced to be

$$\eta_{acc} \approx \frac{I \cdot E_{kin}}{\frac{I^{\frac{2}{3}} \cdot E_{kin}^2}{2 \cdot R \cdot q} + I \cdot E_{kin} + q \cdot P_{aux}}. \quad (2.6)$$

337 As the denominator contains the beam current with an exponent of ≤ 1 the efficiency will
 338 increase with the beam current. With the actual setup of the Ring cyclotron, i.e., cavity voltages
 339 of $V_{acc} = 850$ kV and a beam current of 2.4 mA, the efficiency is 0.18, which is the highest
 340 for any high power accelerator existing to date [42]. By increasing the beam current to the
 341 ultimate goal of 3.0 mA at a cavity voltage of 1 MV an efficiency 0.21 could be achieved. This
 342 is feasible at PSI, since the RF-system is designed for a peak voltage of up to 1.2 MV. The
 343 limitation of 850 kV and thus the maximum beam current is given by the flattop cavity system.
 344 Currently, the maximum flattop voltage is 550 kV corresponding to the necessary 11% of the
 345 main cavity voltage. For an operation at higher voltages the flattop system, including the cavity
 346 and the amplifiers, would have to be replaced. It is important to note, that these values are
 347 valid for the specific setup of the Ring cyclotron, i.e., four accelerating cavities with a given
 348 shunt impedance R . If the acceleration voltage or the energy gain per turn respectively were
 349 distributed among 8 cavities, the wall losses per cavity would be lower. If calculated for eight
 350 cavities, the efficiency would be 0.2 at 2.4 mA. It is obvious that the shunt impedance R is

351 one of the main parameters to optimize the efficiency at a given gap voltage. In fact, the
352 shunt impedance only depends on the geometry and choice of material of the cavity and is,
353 therefore, the parameter to optimize. This is an important consideration for future cyclotron
354 based accelerator driven systems.

355 References

- 356 [1] J. P. Blaser and H. A. Willax, *Progress report on the 500 MeV isochronous cyclotron meson*
357 *factory of eth zurich*, In F. Howard, ed., *4th International Conference on Isochronous Cy-*
358 *clotrons (Cyclotrons '66)*, vol. 13, pp. 194–213. IEEE, ISBN 978-3-95450-098-7 (1966).
- 359 [2] H. A. Willax, *Proposal for a 500 MeV isochronous cyclotron with ring magnet*, In F. Howard
360 and N. Vogt-Nilsen, eds., *CERN Report 63-19*, pp. 386–397. CERN, ISBN 978-3-95450-
361 086-4 (1963).
- 362 [3] H. A. Willax, *Status report on S.I.N.*, In McIlroy [43], pp. 58–72 (1969).
- 363 [4] W. Joho, M. Olivo, T. Stambach and H. Willax, *The SIN accelerators, operational expe-*
364 *rience and improvement programs*, In *Proceedings, 1977 Particle Accelerator Conference:*
365 *Accelerator Engineering and Technology*, vol. 24, pp. 1618–1621. IEEE, New York (1977).
- 366 [5] W. Joho, *The S.I.N. ring cyclotron after one year of operation*, In F. E. Mills, ed., *Proceedings,*
367 *1975 Particle Accelerator Conference, Accelerator Engineering and Technology*, vol. 22, pp.
368 1397–1401. IEEE, New York (1975).
- 369 [6] W. Joho, *Recent and future developments at S.I.N.*, In *Proceedings, 1979 Particle Accelerator*
370 *Conference: Accelerator Engineering and Technology*, vol. 26, pp. 1949–1957. IEEE, New
371 York (1979).
- 372 [7] C. Baumgarten, A. Barchetti, H. Einkenkel, D. Goetz and P. A. Schmelzbach, *A compact elec-*
373 *tron cyclotron resonance proton source for the paul scherrer institute's proton accelerator fa-*
374 *ility*, *Review of Scientific Instruments* **82**(5), 053304 (2011), doi:[10.1063/1.3590777](https://doi.org/10.1063/1.3590777),
375 <https://doi.org/10.1063/1.3590777>.
- 376 [8] Y. Dai and G. S. Bauer, *Status of the first sinq irradiation experiment, stip-i*, *J. Nucl. Mat.*
377 **296**, 43 (2001).
- 378 [9] W. Wagner, J. Mesot, P. Allenspach, G. Kuehne and H. M. Ronnow, *The swiss spallation*
379 *neutron source sinq developments and upgrades for optimized user service*, *Physica B* **385-**
380 **386**, 968 (2006).
- 381 [10] G. S. Bauer, *Operation and development of the new spallation neutron source sinq*
382 *at the paul scherrer institut*, *Nuclear Instruments and Methods in Physics Re-*
383 *search Section B: Beam Interactions with Materials and Atoms* **139**(1), 65 (1998),
384 doi:[https://doi.org/10.1016/S0168-583X\(97\)00956-7](https://doi.org/10.1016/S0168-583X(97)00956-7).
- 385 [11] W. Wagner, Y. Dai, H. Glasbrenner, M. Grosse and E. Lehmann, *Status of sinq, the only*
386 *mw spallation neutron source—highlighting target development and industrial applications*,
387 *Nucl. Instr. Meth. A* **562**(2), 541 (2006).
- 388 [12] B. B. et al, *The swiss spallation neutron source sinq at paul scherrer institut*, *Neutron News*
389 **20**(3), 5 (2009).

- 390 [13] B. Lauss and the PSI UCN Project Team, *Commissioning of the new high-intensity ultra-*
391 *cold neutron source at the paul scherrer institut*, Journal of Physics: Conference Series
392 **312**(052005) (2011).
- 393 [14] B. Lauss, *Startup of the high-intensity ultracold neutron source at the paul scherrer institute*,
394 In P. Bühler, O. Hartmann, K. Suzuki, E. Widmann and J. Zmeskal, eds., *Proceedings of*
395 *EXA 2011*, pp. 297–301. Springer, Dordrecht, Netherlands, ISBN 978-94-007-4890-3
396 (2012).
- 397 [15] B. Lauss, *Ultracold neutron production at the second spallation target of the paul scherrer*
398 *institute*, Physics Procedia **51**, 98 (2014).
- 399 [16] R. M. Bergmann, U. Filges, D. Kiselev, T. Reiss, V. Talanov and M. Wohlmuther, *Upgrades*
400 *to the sinq cold neutron source*, J. of Phys. Conf. Ser. **746**, 012035 (2015).
- 401 [17] A. Kolano, A. Adelman, R. Barlow and C. Baumgarten, *Intensity limits of the PSI injector*
402 *II cyclotron*, Nucl. Instrum. Meth. in Phys. Res. A **885**, 54 (2018).
- 403 [18] M. M. Gordon, *The longitudinal space charge effect and energy resolution*, In McIlroy [43],
404 pp. 305–317 (1969).
- 405 [19] A. Chabert, T. Luong and M. Promé, *Separate sector cyclotrons beam dynamics*, In W. Joho,
406 ed., *Proceedings of the 7th International Conference on Cyclotron and their Applications*,
407 pp. 245–247. Birkhäuser, Basel CH, ISBN 978-3-95450-159-5 (1975).
- 408 [20] C. Chasman and A. J. Baltz, *Space charge effects in a heavy ion cyclotron*, Nucl. Instr.
409 Meth. **219**, 279 (1984).
- 410 [21] S. Adam, *Calculation of space charge effects in isochronous cyclotrons*, In A. Strathdee,
411 ed., *Proceedings of the 1985 Particle Accelerator Conference (PAC1985)*, vol. 32, pp. 2507–
412 2509. IEEE, Piscataway, NJ, doi:[10.1109/TNS.1985.4333654](https://doi.org/10.1109/TNS.1985.4333654) (1985).
- 413 [22] R. Koscielniak and S. Adam, *Simulation of space-charge dominated beam dynamics in*
414 *an isochronous avf cyclotron*, In S. T. Corneliussen and L. Carlton, eds., *Proceedings of*
415 *the 1993 Particle Accelerator Conference (PAC 93)*, pp. 3639–3641. IEEE, Piscataway, NJ,
416 ISBN 9780780312036 (1993).
- 417 [23] S. Adam, *Space charge effect in cyclotrons - from simulations to insights*, In Comell [44],
418 pp. 446–448 (1995).
- 419 [24] J. J. Yang, A. Adelman, M. Humbel, M. Seidel and T. J. Zhang, *Beam dy-*
420 *namics in high intensity cyclotrons including neighboring bunch effects: Model, im-*
421 *plementation, and application*, Phys. Rev. ST Accel. Beams **13**, 064201 (2010),
422 doi:[10.1103/PhysRevSTAB.13.064201](https://doi.org/10.1103/PhysRevSTAB.13.064201).
- 423 [25] E. Pozdeyev, J. A. Rodriguez, F. Marti and R. C. York, *Longitudinal beam dynamics studies*
424 *with space charge in small isochronous ring*, Phys. Rev. ST Accel. Beams **12**, 054202
425 (2009), doi:[10.1103/PhysRevSTAB.12.054202](https://doi.org/10.1103/PhysRevSTAB.12.054202).
- 426 [26] C. Baumgarten, *Transverse-longitudinal coupling by space charge in cyclotrons*, Phys. Rev.
427 ST Accel. Beams **14**, 114201 (2011), doi:[10.1103/PhysRevSTAB.14.114201](https://doi.org/10.1103/PhysRevSTAB.14.114201).
- 428 [27] C. Baumgarten, *Transverse-longitudinal coupling by space-charge in cyclotrons*, In J. Thom-
429 son and V. Schaa, eds., *Proceedings of the 20th International Conference on Cyclotrons and*
430 *their Applications*, pp. 315–319. JaCoW, ISBN 978-3-95450-128-1 (2013).

- 431 [28] C. Baumgarten, *Factors influencing the vortex effect in high-intensity cyclotrons*, In L. Con-
432 radie, J. G. De Villiers and V. R. W. Schaa, eds., *Proceedings of the 22nd International*
433 *Conference on Cyclotrons and their Applications*, pp. 270–274. JACoW, Geneva, Switzer-
434 land, ISBN 978-3-95450-205-9 (2019).
- 435 [29] *SIN annual report*, Swiss Institute for Nuclear Research (S.I.N.), Villigen, Switzerland.
436 (1974).
- 437 [30] *SIN annual report*, Swiss Institute for Nuclear Research (S.I.N.), Villigen, Switzerland.
438 (1975).
- 439 [31] Y. Bi, A. Adelman, R. Dölling, M. Humbel, W. Joho, M. Seidel and T. Zhang, *Challenges*
440 *in simulating mw beams in cyclotrons*, In A. Adelman, J. Chrin, M. Marx, V. R. W. Schaa
441 and M. Seidel, eds., *Proceedings of the 46th ICFA Advanced Beam Dynamics Workshop on*
442 *High-Intensity and High-Brightness Hadron Beams (HB2010)*, pp. 295–299. PSI, Villigen,
443 Switzerland (2011).
- 444 [32] W. Joho, *High intensity problems in cyclotrons*, In G. Gendreau, ed., *Proceedings of the 9th*
445 *International Conference on Cyclotron and their Applications*, pp. 337–47. Les Editions de
446 Physique, BP 112, 91402 Orsay (France), ISBN 978-3-95450-160-1 (1981).
- 447 [33] T. Stambach, S. Adam, H. R. Fitze, W. Joho and U. Schryber, *Potential of cyclotron based*
448 *accelerators for energy production and transmutation*, Int. Conf. on Acc.-Driven Transmut.
449 Techn. and Appl. pp. 229–235 (1995), doi:[10.1063/1.49093](https://doi.org/10.1063/1.49093), AIP Conf. Proc. 346, 1995.
- 450 [34] U. Schryber, S. Adam, T. Blumer, J. Cherix, H. Fitze, H. Frei, D. George, G. Heidenreich,
451 M. Humbel, I. IIROUSEK, W. Joho, M. Marki *et al.*, *High power operation of the PSI*
452 *accelerators*, In Comell [44], pp. 32–35 (1995).
- 453 [35] W. Joho, *High intensity beam acceleration with the SIN cyclotron facility*, In M. Sekiguchi,
454 Y. Yano and K. Hatanaka, eds., *Proceedings of the 11th International Conference on Cy-*
455 *cyclotron and their Applications*, pp. 31–37. Ionics Publ., Tokyo (1987), ISBN 978-3-95450-
456 166-3 (1986).
- 457 [36] J. Stetson, S. Adam, M. Humbel, W. Joho and T. Stambach, *The commissioning of PSI*
458 *injector 2 for high intensity, high quality beams*, In G. Dutto and M. Craddock, eds.,
459 *Proceedings of the 13th International Conference on Cyclotrons and their Applications*, pp.
460 36–39. World Scientific (1993).
- 461 [37] J. Grillenberger, M. Humbel, J. Y. Raguin and P. A. Schmelzbach, *Commissioning of the*
462 *new buncher system in the 870 keV injection beamline*, In Refuggiato [45], pp. 464–466
463 (2007).
- 464 [38] M. Seidel and P. Schmelzbach, *Upgrade of the psi cyclotron facility to 1.8 mw*, In Refuggiato
465 [45], pp. 157–162 (2007).
- 466 [39] M. Seidel, J. Grillenberger and A. Mezger, *High intensity operation and control of beam*
467 *losses in a cyclotron based accelerator*, In N. Zhao, J. Chrin, V. R. W. Schaa, C. Petit-Jean-
468 Genaz, D. Ji and H. Yan, eds., *Proceedings of the 52nd ICFA Advanced Beam Dynamics*
469 *Workshop on High-Intensity and High-Brightness Hadron Beams (HB2012)*, JACoW con-
470 ferences, pp. 555–559. JACoW, Geneva, Switzerland (2013).
- 471 [40] Y. J. Bi, A. Adelman, R. Dölling, M. Humbel, W. Joho, M. Seidel and T. J. Zhang, *Towards*
472 *quantitative simulations of high power proton cyclotrons*, Phys. Rev. ST Accel. Beams **14**,
473 054402 (2011).

- 474 [41] A. Kovach, A. Parfenova, J. Grillenberger and M. Seidel, *Energy efficiency and saving*
475 *potential analysis of the high intensity proton accelerator HIPA at PSI*, Journal of Physics:
476 Conference Series **874**, 012058 (2017).
- 477 [42] J. Grillenberger, S.-H. Kim, M. Yoshii, M. Seidel and V. Yakolev, *The energy efficiency*
478 *of high intensity proton driver concepts*, In V. R. W. Schaa, G. Arduini, M. Lindroos and
479 J. Pranke, eds., *Part 2, Proceedings of the 8th International Particle accelerator Conference*
480 *(IPAC 2017)*, vol. 874, pp. 4842–4847. JACoW, Geneva, Switzerland (2017).
- 481 [43] R. McLroy, ed., *Proceedings of the 5th International Conference on Cyclotrons and their*
482 *Applications*. Butterworth London (1971), ISBN 978-3-95450-102-1 (1969).
- 483 [44] J. Comell, ed., *14th International Conference on Cyclotrons and their Applications*. World
484 Scientific (1995).
- 485 [45] D. Refuggiato, ed., *18th International Conference on Cyclotrons and their Applications*.
486 INFN - LNS Catania, Italy (2008), ISBN 978-3-95450-041-3 (2007).